Desalination and Water Treatment
www.deswater.com

doi: 10.5004/dwt.2019.23432

142 (2019) 114–124
February

Effects of inorganic nanoparticle/PEG600 composite additives on properties of chlorinated polyvinyl chloride ultrafiltration membranes

Wei Zhang, Honghai Yang*, Jun Wang*

College of Environmental Science and Engineering, Donghua University, Shanghai 201620, China, emails: Wangj@dhu.edu.cn (J. Wang), yhh@dhu.edu.cn (H. Yang), ReviewReview@163.com (W. Zhang)

Received 12 March 2018; Accepted 7 November 2018

ABSTRACT

To enhance the hydrophilicity and antifouling property of chlorinated polyvinyl chloride (CPVC), ultrafiltration (UF) membrane used in water treatment process, inorganic nanoparticles (nano-Al_2O_3, nano-TiO_2, nano-ZnO, and nano-SiO_2), polyethyleneglycol (PEG), and nanoparticle/PEG composite additives were blended with CPVC and investigated for their casting dope viscosity. Effects of these additives on the CPVC UF membranes were characterized by scanning electron microscopy, filtration studies, contact angle, and mechanical property. The results show that the addition of 3 wt.% nanoparticles leads to membranes with lower pure water flux (PWF), lower rejection, and higher flux recovery ratio (FRR). However, with the addition of PEG in CPVC/nanoparticle membranes, PWF and rejection were restored. Meantime, FRR further increased and mechanical properties decreased. CPVC UF membranes incorporated with nano-Al_2O_3/PEG possessed comprehensive merits, including higher PWF, lowest contact angle, and best antifouling property compared with other CPVC UF membranes used in this paper.

Keywords: CPVC ultrafiltration membrane; Composite additive; Hydrophilicity; Antifouling property

1. Introduction

Membrane separation technology, as an emerging technique, had been used in various industry fields, such as chemical engineering, food, pharmacy, water, wastewater treatment, and so on, due to its high separation efficiency, easy to operate, and cost effectiveness. However, membrane fouling, owing to the adsorption of protein, polysaccharide, humic acid, etc. in the membrane filtration process, will result in the sharp decrease of flux, which resulted in the increased membrane cleaning ratio and decline in the life span of membrane, further making the membrane replacement rate increase, and at last led to the cost of membrane separation increase dramatically. So the membrane fouling was the bottle neck of the widespread application of membrane separation technology [1]. Many researches showed that the hydrophobicity of the membrane made the membrane incline to adsorption materials resulting in membrane fouling. This result means that improving the hydrophilicity of membranes can solve the membrane fouling effectively.

Up to date, the reported methods to improve the membrane hydrophilicity included blending with nanoparticle (nano-Al_2O_3, nano-TiO_2, nano-ZnO, nano-SiO_2, etc.), hydrophilic polymer, or composite additive nanoparticle and surface active agent (for example, Al_2O_3/PEG400, SiO_2/PEG600), surface coating, functional group grafting, and so on. Among these methods, the blending with nanoparticle (nano-Al_2O_3, nano-TiO_2, nano-ZnO, nano-SiO_2, etc.) was used in many hydrophilic modifications of membranes by scholars. This was because not only the hydrophilicity of membranes was improved apparently but also the mechanical properties were consolidated due to the enhanced thermal stability; the formation of macropores in the membrane was suppressed only by a small amount of nanoparticle [2–4]. Furthermore, this method had the merits of simplicity, mild condition, and easy to operate. Maximous et al. [5] added

* Corresponding author.

Al_2O_3 to polyethersulfone (PES) membranes and demonstrated lower flux decline during activated sludge filtration compared with neat polymeric membrane. They suggested that the hydrophobic interaction between the membrane surface and foulants was an important factor affecting the antifouling property of the membranes.

Bazargan et al. [6] prepared poly (vinylidene fluoride) (PVDF) membranes by phase-inversion process, and the results indicated that the addition of nano-Al_2O_3 to the casting dope increased the hydrophilicity of the PVDF membrane surface. Lu et al. [7] prepared nanocomposite tubular ultrafiltration (UF) membrane Al_2O_3-PVDF via the phase-inversion method, and the results showed that the addition of nano-Al_2O_3 improved membrane antifouling property, and the flux recovery ratio (FRR) of modified membranes reached 100% washing with 1 wt.% of OP-10 surfactant solution (pH 10), which was attributed to the membrane hydrophilicity improvement due to the addition of nano-Al_2O_3 into the PVDF. Garcia-Ivars et al. [8] modified commercial flat-sheet PES membranes with a nominal molecular weight and the results indicated that PES/Al_2O_3 membranes displayed superior antifouling properties and rejection values. They suggested that the presence of Al_2O_3 nanoparticles on the membrane surface reduced the interactions between organic compounds and surface material, due to the higher affinity of Al_2O_3 for water than PES material. Mehrnia et al. [9] synthesized Al_2O_3/polysulfone (PSf) nanocomposite membrane by blending method, and the results showed that filtration resistances especially cake resistance and total resistance diminished as the nano-Al_2O_3 particles increased. They suggested that nanoparticles played a great role in membrane fouling reduction. Damodar et al. [10] prepared the nanocomposite membrane of PVDF/TiO_2 by phase-inversion method, and the 1%–4% PVDF/TiO_2 membranes showed lower contact angles as compared with neat PVDF membranes due to the increase in hydrophilicity by TiO_2 addition. Wang et al. [11] prepared PVDF/TiO_2 composite membranes by a phase-inversion method and demonstrated the improvement of the antifouling ability, which was attributable to the increased repulsive interaction energy barrier between foulants and membrane surfaces. Sotto et al. [12] manufactured blended PSf/TiO_2 flat-sheet membranes and studied membrane fouling with humic acids as model organic foulants. The results showed that the fouling of the TiO_2-entrapped membrane was minimized, which was due to the decreased probability of hummic acid adsorbed on the membrane surface with the hydrophilicity increased. Qin et al. [13] prepared a highly hydrophilic PVDF membrane via binding of TiO_2 nanoparticles, and the FRR was apparently increased from 20.0% to 80.5%, which was mainly ascribed to the improvement of surface hydrophilicity. Mishra et al. [14] prepared a Poly(1,4-phenylene ether ether sulfone)/TiO_2 composite UF membrane via a phase-inversion method, and the antifouling property was improved due to the presence of nano-TiO_2 particles and increased the surface hydrophilicity. Hong et al. [15] reported a novel photocatalytic PVDF UF membrane via phase-inversion method. The experiments indicated that the block resistance decreased with an increase in nano-ZnO content owing to the improvement in the membrane hydrophilicity. Balta et al. [16] manufactured PES membranes via diffusion-induced phase inversion in N-methylpyrrolidone, and the results showed that ZnO-blended membrane showed lower flux decline due to a higher hydrophilicity of the ZnO membranes. Shen et al. [17] prepared PES membranes and ZnO/PES hybrid membranes by a phase-inversion method. The experiments indicated when the weight of the added nano-ZnO is 0.3 g, the decreased flux ratio of the ZnO/PES hybrid membrane was only 7.8% after 90 min of filtering, whereas the decreased flux ratio of the PES membrane was 27.7%. They suggested that the presence of nano-ZnO particles increased the surface hydrophilicity. Jafarzaden et al. [18] fabricated high-density polyethylene (PE) membranes embedded with ZnO nanoparticles via thermally induced phase separation method. The results indicated that incorporation of nano-ZnO into PE membranes not only increased fouling resistance but also decreased irreversible fouling, which might be attributed to the fact that the presence of nano-ZnO on the surface of membranes increased hydrophilicity. Zhao et al. [19] fabricated PES/ZnO membranes with wet phase separation. The results indicated that PES/ZnO membranes exhibited lower contact angles. They suggested that the improvement in surface hydrophilicity of PES/ZnO membranes might be ascribed to the incorporated hydrophilic nano-ZnO. Additionally, Yu et al. [20] reported that a novel low-cost SiO_2/polyvinyl chloride (PVC) membrane was prepared by the phase-inversion process and demonstrated better capabilities against protein absorption and higher water flux ratio, as a hydrophilic layer was formed on the surface and the cross section of the modified membrane with the addition of nano-SiO_2. Habibi et al. [21] prepared hybrid PSf UF membrane using phase-inversion method, and the results indicated that the addition of SiO_2 nanoparticles significantly improved fouling resistance of the membrane. These might be due to the surface hydrophilicity enhancement which restrained the adsorption of bovine serum albumin (BSA). Shen et al. [22] prepared PES/SiO_2 composite membranes via phase-inversion method. The results showed that the membrane structure was not significantly affected by the addition of SiO_2; the hydrophilicity and antifouling were enhanced by adding SiO_2 nanoparticles. Huang et al. [23] prepared PVDF/SiO_2 hybrid UF membranes via phase inversion by a tetraethoxysilane (TEOS) sol-gel process. The experimental data indicated that hydrophilicity, permeation, rejection, porosity, and mean pore size of the hybrid membranes increased with ascending TEOS contents. Zhu et al. [24] prepared hybrid PVDF UF membranes via nonsolvent-induced phase separation through blending zwitterionic SiO_2 nanoparticles. The results showed that the addition of zwitterionic SiO_2 nanoparticles inhibited the irreversible fouling of the membrane through improving the hydrophilicity.

However, nanoparticles agglomerate easily, which exerts blocking effect on membrane pores, leading to reduced water flux of the membrane. Maximous et al. [5] reported that as the Al_2O_3 contents increased, the possibility of pore plugging increased resulting in decreased water flux. Li et al. [25] prepared hollow mesoporous silica spheres (HMSS)/PSf composite UF membrane, and the experimental data indicated that the pure water flux (PWF) first increased with fraction of HMSS in the membrane matrix up to 1.5% and then decreased at a fraction of 2% owing to particle agglomeration and pore blockage. Lu et al. [26] prepared PVDF UF membrane modified by nano-Al_2O_3 and the results showed

that the membranes consisted of more amounts nanosized Al_2O_3 particles, as its flux could not be improved, which was attributed to the phenomena of reunion of the nano-Al_2O_3 particles. Liu et al. [27] prepared PVDF-based UF membranes using nano-γ-Al_2O_3, and the experimental data showed that higher concentration of nano-γ-Al_2O_3 resulted in lower flux, which is caused by the blocking of the membrane pores of the excess nano-γ-Al_2O_3. Rabiee et al. [28] prepared PVC UF membranes by incorporation of nano-ZnO. They observed that the PWF increased continuously with the addition of nano-ZnO up to 3 wt.%, and then it decreased as ZnO nanoparticles were more likely to aggregate and cause pore blockage at membrane surface. In order to prepare membranes with larger flux, scholars mix nanoparticles (such as nano-Al_2O_3, nano-TiO_2, nano-ZnO, nano-SiO_2, etc) with surface active agent including polyethyleneglycol (PEG), polyvinyl pyrrolidone, and F127 according to different proportions so as to produce the composite additives that are added into the casting solution. Hydrophilic nanoparticles can enhance the hydrophilicity, antifouling property, and mechanical property of the membrane; surface active agent on one hand can weaken the surface tension of the casting solution, facilitating the uniform dispersion of nanoparticles [29]; on the other hand, it can be used as pore-formation agent, improving the porosity of the membrane. Garcia-Ivars et al. [30] prepared PES membranes by adding Al_2O_3 and PEG400 as additives to the casting solution. It was observed that the PES/Al_2O_3/PEG400 membranes displayed superior antifouling properties and desirable UF properties as addition of Al_2O_3/PEG resulted in the formation of a hydrophilic finger-like structure with macrovoids. Song et al. [1] observed the enhanced self-cleaning ability of PVDF membranes with the addition of TiO_2 and PEG600 as additives, which was probably due to the smaller contact angle of PVDF-TiO_2-PEG membrane and thus more hydrophilic property of membrane. Similarly, Ali et al. [31] obtained increased separation factor and high permeation flux for cellulose acetate (CA) membranes when ZnO and PEG600 were added as additives. The increased separation factor was attributed to the hydrophilic effect of CA/ZnO and the high permeation flux could be explained by the plasticizing effect of PEG600, resulting in an increased flexibility of polymer chains, and consequently, the hydrophilic structure formed might give higher permeation flux. Further, Arthanareeswaran et al. [32] found that the presence of pore formers (PEG600 and LiCl) in the composition CA/SiO_2 blend membrane improve the FRR due the decrease of the total fouling resistance.

In particular, chlorinated polyvinyl chloride (CPVC) is prepared through deep chlorination of PVC, which not only owns the excellent chemical stability, acid and alkali resistance, and corrosion resistance of PVC but also possesses great mechanical property and better thermal stability. Furthermore, it is cheap and easy to be prepared. Thus, it has attracted the attention of scholars in the preparation field of membrane materials [33]. However, the hydrophobicity of CPVC UF membrane is strong so it can be easily polluted during the use process. Thus, the hydrophilicity of CPVC UF membrane needs to be modified.

As for the research on the effect of nanoparticle/PEG composite additive on the property of CPVC UF membrane, there has not been any literature yet. Thus, in this paper, it is intended that different composite additives are produced through combination of nano-Al_2O_3, nano-TiO_2, nano-ZnO, nano-SiO_2, and PEG. By comparing the effects of the four composite additives on the property of CPVC UF membrane, the composite additive containing the most appropriate nanoparticle is confirmed.

2. Experiment

2.1. Materials and instruments

CPVC (degree of polymerization = 1,000) was provided by Chlor-Alkali Chemical Co. Ltd. (China). *N*,*N*-dimethylacetamide (DMAC) was purchased from Pharmaceutical (Group) Chemical Reagent Co. (China). Nano-Al_2O_3, nano-TiO_2, nano-ZnO, and nano-SiO_2 were purchased from Wanjing New Material Co. (China), size of the composites is 30 ± 5 nm; PEG600 was purchased from Sigma-Aldrich Co. (Shanghai, China), BSA (molecular weight = 67,000) was produced by Sigma-Aldrich Co (Shanghai, China).

Rotating viscometer (DNJ-1, Jinghai, China), scanning electron microscopy (SEM; JSM-5600LV, Japan), filtration cell (MSC300, China), contact-angle meter (SL200C, Solon, China), total organic carbon analyzer (TOC-VCPN, Shimadzu, Japan), material testing machine (H5K-S, United Kingdom) were all used.

2.2. Casting solution and membrane preparation

With CPVC as the main membrane material, neat CPVC membrane and modified CPVC membrane were prepared by phase-inversion method. The solutions consisting of CPVC and DMAC as well as inorganic and organic additives were cast onto a clean glass plate at 90°C. After casting, the liquid membranes with the glass plate were immersed into distilled water coagulation bath at 35°C immediately. The characterization of the membranes was carried out, and the membranes were further immersed in 0.1% $NaHSO_3$ solution for 24 h. Compositions of casting solution are shown in Table 1.

2.3. Measurements of the shear viscosity of the casting solution

The shear viscosity was measured by rotating viscometer (DNJ-1, Jinghai, China).

2.4. Membrane characterization

2.4.1. Observation of membrane morphology

The cross section and surface morphologies of the membranes were observed by SEM (JSM-5600LV, Japan). The membranes were frozen in liquid nitrogen, broken, and sputtered with gold before SEM analysis.

2.4.2. PWF and rejection ratio measurements

2.4.2.1. PWF measurements

In this study, a 300-mL stirred batch cell experimental setup was used for the permeability experiments, which is

Table 1
Compositions of casting solution

Membranes	CPVC/wt.%	Al_2O_3/wt.%	TiO_2/wt.%	ZnO/wt.%	SiO_2/wt.%	PEG/wt.%	DMAC/wt.%
CPVC	18	–	–	–	–	–	82
CPVC/PEG	18	–	–	–	–	8	74
CPVC/Al_2O_3	18	3	–	–	–	–	79
CPVC/Al_2O_3/PEG	18	3	–	–	–	5	74
CPVC/TiO_2	18	–	3	–	–	–	79
CPVC/TiO_2/PEG	18	–	3	–	–	5	74
CPVC/ZnO	18	–	–	3	–	–	79
CPVC/ZnO/PEG	18	–	–	3	–	5	74
CPVC/SiO_2	18	–	–	–	3	–	79
CPVC/SiO_2/PEG	18	–	–	–	3	5	74

presented schematically in Fig. 1. The membrane was placed in MSC cup ultrafilter for 40 min before loading at 0.10 MPa. Subsequently, its PWF was measured at 0.10 MPa, and the filtrate volume prepared by one-time filtration was tested every 10 min for 60 min. The calculation formula [15] of flux (J_{w1}; L m^{-2} h^{-1}) is shown as Eq. (1):

$$J_{w1} = \frac{V}{At} \tag{1}$$

where V, A, and t represent the volume of permeated water (L), the membrane filtering area (m^2), and the permeation time (h), respectively.

2.4.2.2. Rejection measurements

The same unit was fed with a 1.0-mg mL^{-1} BSA (molecular weight = 67,000) solution for the rejection experiment at a stirring speed of 300 rpm and room temperature. Then, the protein concentrations (mg L^{-1}) of both the feed (C_f) and the permeate solution (C_p) were determined with a total organic carbon analyzer (TOC-VCPN, Shimadzu) at an operating pressure of 0.10 MPa for 60 min. The calculation formula [15] of BSA rejection ratio (R; %) was shown as Eq. (2):

$$R = \frac{C_f - C_p}{C_f} \times 100\% \tag{2}$$

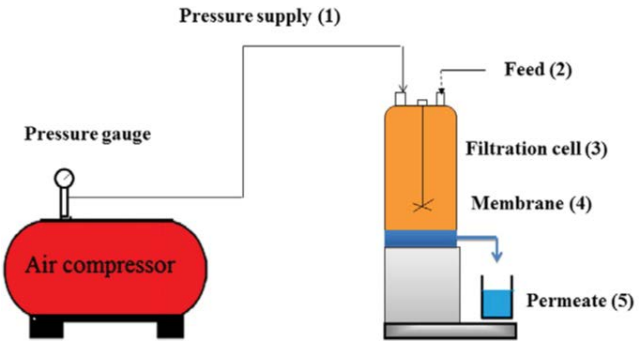

Fig. 1. Schematic diagram of the batch cell ultrafiltration setup.

2.4.3. Contact-angle measurements

The contact angles were measured with a contact-angle meter (SL200C, Solon) at room temperature. Five microliters of water was dropped on the top surface of a dry membrane from a microsyringe with a stainless steel needle. The static contact angle was obtained by measurement of the average value of contact angles measured ten times at different places on the membrane sample.

2.4.4. Characterization of antifouling property

The membrane-simulated crossflow, realized by constant vigorous stirring in a dead-end filtration device connected with an air compressor pump and solution reservoir, was designed to characterize the filtration performance of the membranes. The membrane was first precompacted at a transmembrane pressure of 0.10 MPa with distilled water for 40 min. Subsequently, its PWF was measured at 0.10 MPa, and the filtrate volume prepared by one-time filtration was tested every 10 min for 60 min. Then, the attenuation experiments were conducted with a BSA solution from an aeration tank as the feed needed to achieve quick and severe fouling on the membranes. The permeate flux of the BSA solution (J_{BSA}) was also recorded at a constant transmembrane pressure of 0.10 MPa and room temperature for 60 min. Afterward, the membrane was dismounted from the cell, and the surface dirt was removed with a brush and sufficiently rinsed with running water. Afterward, a backwash was performed at a transmembrane pressure of 0.15 MPa for 40 min, and the after-cleaning PWF (J_{w2}) was measured in a similar way as described earlier. The FRR was determined by the following equation [13]:

$$\mathrm{FRR} = \frac{J_{w2}}{J_{w1}} \times 100\% \tag{3}$$

A higher FRR indicated preferable antifouling properties of the UF membranes. To analyze the fouling process in detail, several resistance ratios were defined to describe the fouling resistance of the blend membranes. The total fouling ratio (R_t), reversible fouling ratio (R_r), and irreversible fouling ratio (R_{ir}) were determined by the following equations [13]:

$$R_t = \left(1 - \frac{J_{BSA}}{J_{w1}}\right) \times 100\% \quad (4)$$

$$R_r = \left(\frac{J_{w2} - J_{BSA}}{J_{W1}}\right) \times 100\% \quad (5)$$

$$R_{ir} = \frac{J_{w1} - J_{w2}}{J_{W1}} \times 100\% \quad (6)$$

2.4.5. Mechanical property measurements

The mechanical property of the membranes was evaluated with a material testing machine (H5K-S, United Kingdom) with a stretching ratio of 20 mm min^{-1} at room temperature. Each specimen was cut into a 5 × 1 cm^2 piece, and the testing of each sample was repeated ten times. The tensile strength (N) and the maximum elongation (mm) were then measured to investigate the effect of the composite additives on the mechanical property of CPVC UF membrane.

3. Results and discussion

3.1. Shear viscosity of the casting solution

Shear viscosity of the casting solution exerts important effects on the microstructure and other properties of the membrane. Shear viscosity influences the diffusion ratio between the solvent and the nonsolvent. When shear viscosity of the casting solution is small, the diffusion ratio between the solvent and the nonsolvent is large, easily resulting in liquid-solid split-phase and sponge-like structure; when shear viscosity of the casting solution is large, the diffusion ratio between the solvent and the nonsolvent is small, easily leading to liquid-liquid split-phase and finger-like porous structure.

Fig. 2 presents the shear viscosity of neat CPVC casting solution and all the modified casting solutions with different additives. As shown in Fig. 2, the additives can increase the shear viscosity of neat CPVC casting solution. As for its causes, on one hand, the percentage contents of solvent decrease with the addition of additives (nanoparticles and PEG); on the other hand, with the addition of additives (nanoparticles and PEG), binding occurs to additive molecular chains and CPVC polymer chains [34]. The nano-Al_2O_3/PEG composite additive and the nano-SiO_2/PEG composite additive can increase more shear viscosity of neat CPVC casting solution while the nano-SiO_2/PEG composite additive can increase the shear viscosity of neat CPVC casting solution the most. The phenomenon may be related to the molecular volume and molecular structure of nanoparticles (Figs. 3(a)–(d)). The molecular volume of Al_2O_3 is the largest while the molecular structure of SiO_2 is stereoscopic structure, which easily leads to binding with polymer chains. Thus, the shear viscosities of CPVC/Al_2O_3/PEG casting solution and CPVC/SiO_2/PEG casting solution increase more.

3.2. Membrane structure and morphology

The structure and morphology of the cross section and surface of neat CPVC membrane and all the modified membranes with different additives are shown in Figs. 4 and 5. As shown in Figs. 4 and 5, all the membranes have asymmetric structure and dense and nonporous surface. And it can be seen that the membranes containing PEG exhibited evident differences in comparison with those which do not contain PEG.

The supporting layers of neat CPVC membrane consist of cone hole and sponge-like structure. The supporting layers of CPVC/Al_2O_3 membrane, CPVC/TiO_2 membrane, CPVC/ZnO membrane, and CPVC/SiO_2 membrane consist of small but uniform finger-like pores on the upper layers and large finger-like pores on the lower layers. The supporting layers of CPVC/PEG membrane consist of sponge-like structure. The supporting layers of CPVC/Al_2O_3/PEG membrane and CPVC/SiO_2/PEG membrane consist of small but uniform finger-like pores on the upper layers and large finger-like pores on the lower layers. But small finger-like

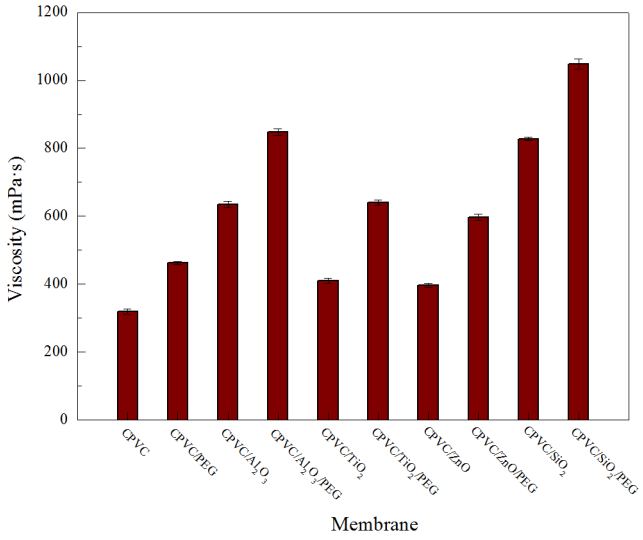

Fig. 2. Shear viscosity of neat CPVC casting solution and modified casting solution.

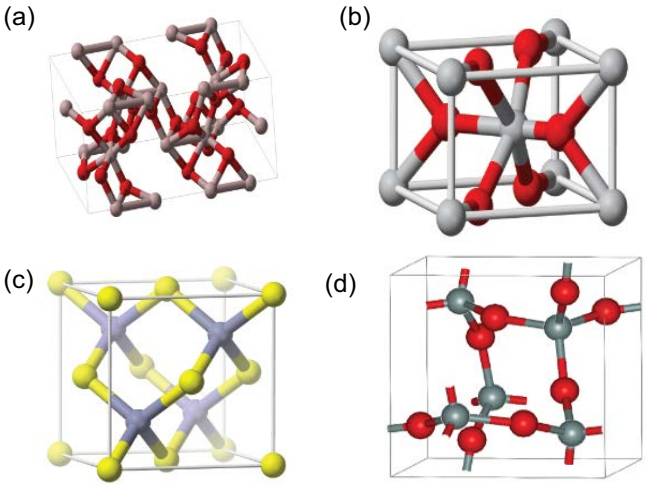

Fig. 3. Molecular structure of (a) Al_2O_3, (b) TiO_2, (c) ZnO, and (d) SiO_2.

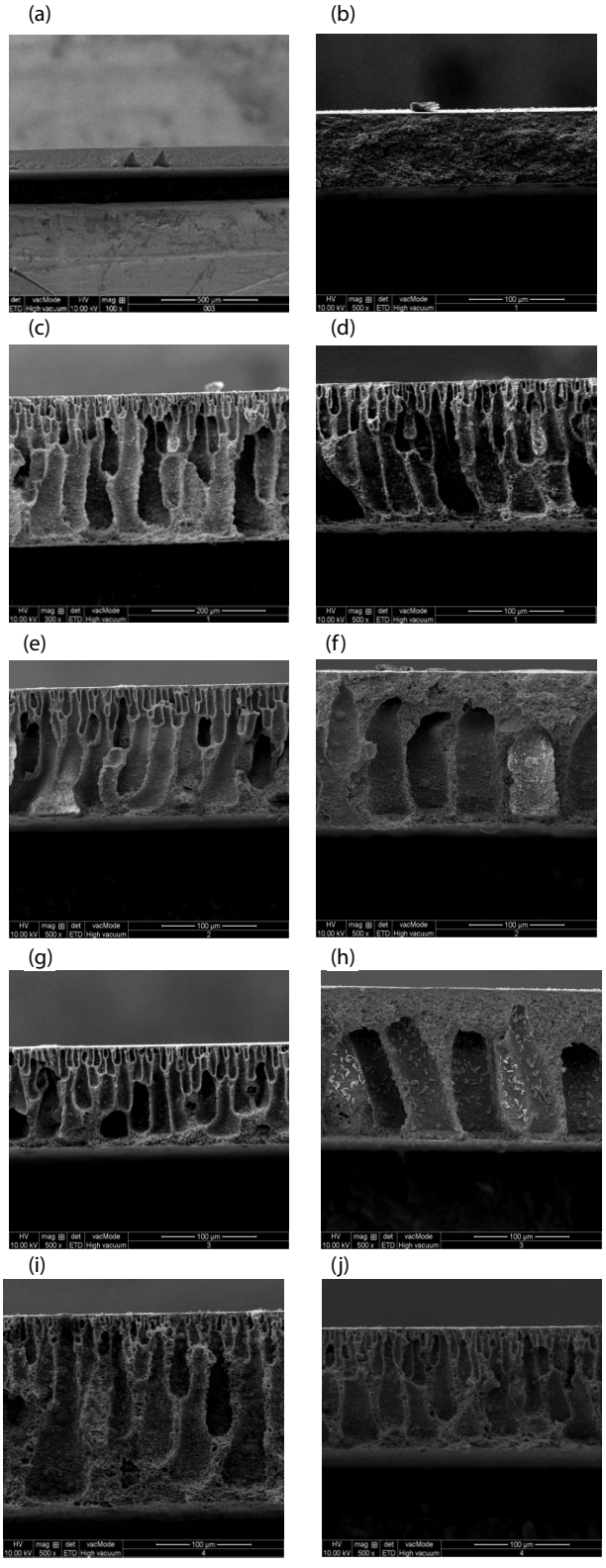

Fig. 4. Cross section of (a) CPVC membrane, (b) CPVC/PEG membrane, (c) CPVC/Al_2O_3 membrane, (d) CPVC/Al_2O_3/PEG membrane, (e) CPVC/TiO_2 membrane, (f) CPVC/TiO_2/PEG membrane, (g) CPVC/ZnO membrane, (h) CPVC/ZnO/PEG membrane, (i) CPVC/SiO_2 membrane, and (j) CPVC/SiO_2/PEG membrane.

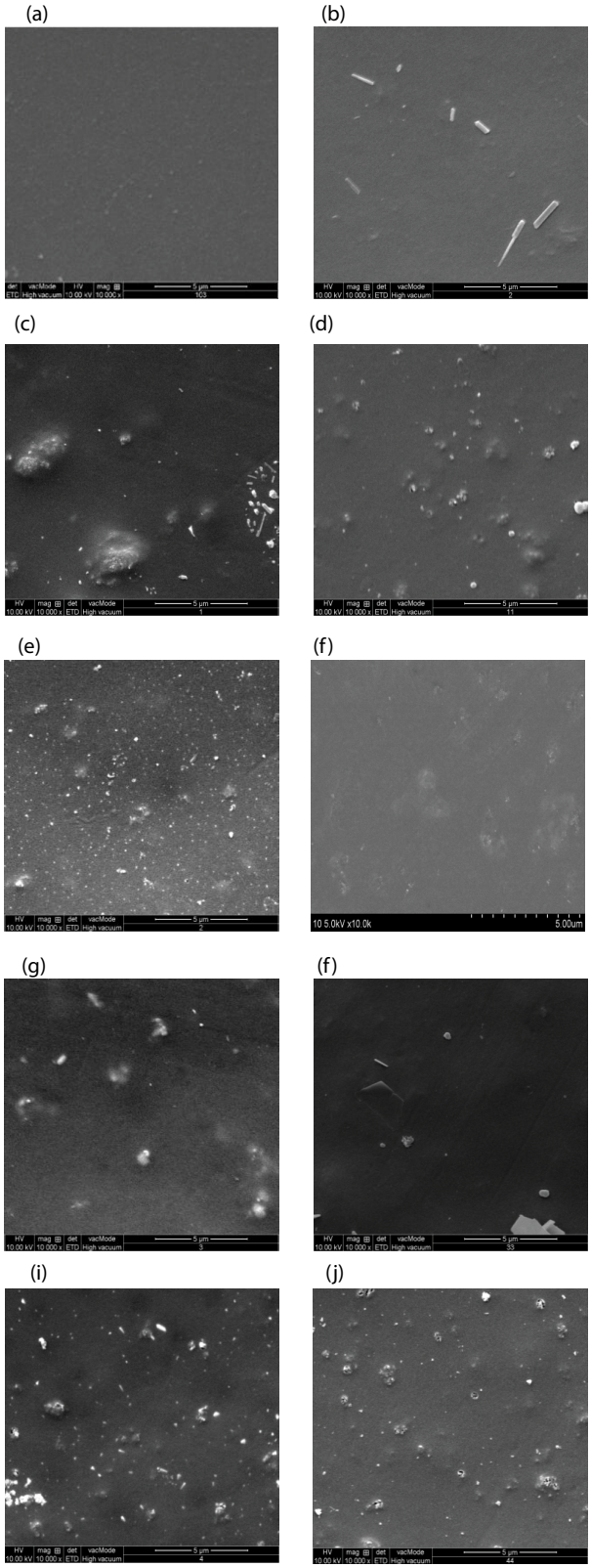

Fig. 5. Surface of (a) CPVC membrane, (b) CPVC/PEG membrane, (c) CPVC/Al_2O_3 membrane, (d) CPVC/Al_2O_3/PEG membrane, (e) CPVC/TiO_2 membrane, (f) CPVC/TiO_2/PEG membrane, (g) CPVC/ZnO membrane, (h) CPVC/ZnO/PEG membrane, (i) CPVC/SiO_2 membrane, and (j) CPVC/SiO_2/PEG membrane.

pores of CPVC/Al_2O_3/PEG membrane and CPVC/SiO_2/PEG membrane became larger in comparison with that of CPVC/Al_2O_3 membrane and CPVC/SiO_2 membrane. The supporting layers of CPVC/TiO_2/PEG membrane and CPVC/ZnO/PEG membrane consist of sponge-like structure on the upper layers and large finger-like pores on the lower layers. As for the emergence of these phenomena, on one hand, PEG600 has an affinity to water. So it is easy to flow out into coagulation bath. According to the general theory of pore formation, this rapid outflow ratio offers macrovoid-free porous interconnecting channels of the sponge-type (I) [35]. On the other hand, the increase in the shear viscosity of the casting solution leads to the diffusion ratio reduction of solvent and nonsolvent, speed reduction of membrane formation, and causes the emergence of liquid-liquid phase separation mechanism, thus large pores appear (II) [36,37]. There are antagonistic effects in these two aspects. When the influence of (I) is greater than that of (II), a sponge-like structure with porous interconnecting channels appears on the membrane cross section; when the influence of (II) is greater than that of (I), the finger-like structure appears on the membrane section; when the influences of (I) and (II) are approximately the same, the change in the membrane cross section is not obvious.

At the same time, Fig. 3 shows that the shear viscosity of CPVC/Al_2O_3/PEG casting solution and CPVC/SiO_2/PEG casting solution is significantly higher than that of CPVC/TiO_2/PEG membrane and CPVC/ZnO/PEG membrane. From Fig. 2, it can be seen that the CPVC/Al_2O_3/PEG membrane and CPVC/SiO_2/PEG membrane cross sections are still indeed finger-like structures because the influences of (I) and (II) are approximately the same, while the CPVC/TiO_2/PEG membrane and CPVC/ZnO/PEG membrane cross sections show sponge-like structures because the influence of (I) is greater than that of (II).

Nanoparticles can be seen on the surfaces of membranes containing nanoparticle.

At the same time, we can see that the surfaces of CPVC/Al_2O_3/PEG membrane, CPVC/TiO_2/PEG membrane, CPVC/ZnO/PEG membrane, and CPVC/SiO_2/PEG membrane have fewer large particles in comparison with those of CPVC/Al_2O_3 membrane, CPVC/TiO_2, CPVC/ZnO, and CPVC/SiO_2 membrane. This result may be due to the fact that the PEG weakens the surface tension of the casting solution, facilitating the uniform dispersion of nanoparticles.

3.3. PWF and rejection

The PWF and rejection of neat CPVC membrane and all the modified membranes with different additives are shown in Fig. 6. As shown in Fig. 6, PWF and rejection of neat CPVC membrane decreased after adding nanoparticles. The reduction in PWF may be explained by the pore blockage at membrane surface that results from the aggregation of nanoparticles as the amount of the nanoparticle reaches 3 wt.%. And the reduction of rejection is also related to the nanoparticle aggregation, which blocks surface pores, in particular, smaller pores; therefore, more large pores are active, and this leads to the reduction in rejection [37–39]. However, PWF and rejection of CPVC membrane increased after adding PEG. The increase of PWF may be due to the higher

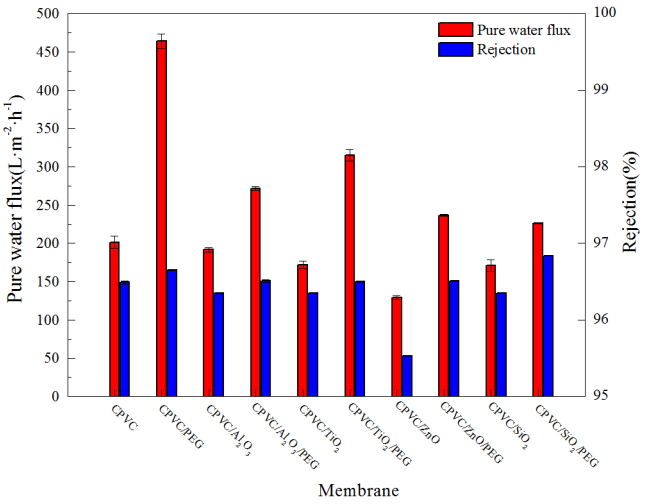

Fig. 6. Pure water flux and rejection of neat CPVC membrane and all the modified membranes with different additives.

interconnected degree of sponge-like pores. Meanwhile, PWF and rejection of CPVC/Al_2O_3 membrane, CPVC/TiO_2 membrane, CPVC/ZnO membrane, and CPVC/SiO_2 membrane increased after adding PEG. As for its causes, on one hand, the higher interconnected degree of sponge-like pores leads to the increment in PWF. On the other hand, PEG weakens the surface tension of the casting solution, facilitating the uniform dispersion of nanoparticles, reducing the pore blockage at membrane surface, which leads to the increased PWF; particularly, reduction of the smaller pore blockage means that less large pores are active, and this leads to increment in rejection.

From Fig. 6, it can be seen that CPVC/PEG membranes have the highest the PWF. As for its causes, on the one hand, CPVC/PEG membranes do not contain nanoparticles, and there is no agglomeration of the particles on the membrane surface from Fig. 6(b). Therefore, the membrane surface is not blocked by the nanoparticle clusters; so the flux is large; on the other hand, the addition of PEG causes the formation of sponge structure without large voids and having porous interconnecting channels. The voids of the sponge-like structure are more interconnected, and the PEG content in the CPVC/PEG membrane is 8%, while the PEG content in the CPVC membrane is 0%, and the PEG content in the CPVC/nanoparticle/PEG membrane is 5%, so the CPVC/PEG membrane has the highest the PWF.

3.4. Hydrophilicity

In this paper, contact angle is used to represent the membrane hydrophilicity. The smaller the contact angle is, the better the membrane hydrophilicity.

The contact angles of neat CPVC membrane and all the modified membranes with different additives are shown in Fig. 7. As shown in Fig. 7, contact angle of neat CPVC membrane decreased after adding nanoparticles. This is due to the hydrophilic nature of nanoparticles which are present on the membranes surfaces. And contact angle of neat CPVC membrane hardly changed after adding PEG. As for

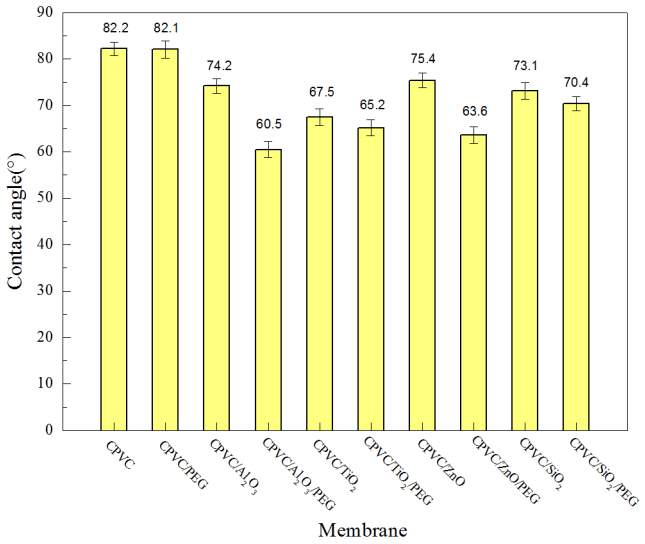

Fig. 7. Contact angle of neat CPVC membrane and all the modified membranes with different additives.

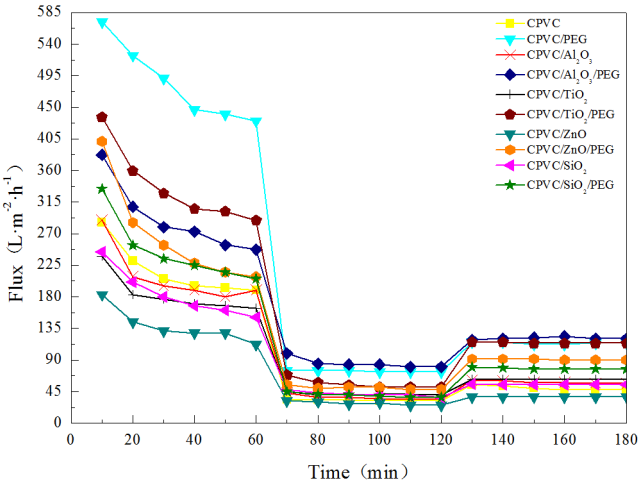

Fig. 8. Flux of pure water and BSA in three 60-min sections: first for pure water, second for BSA, and third for pure water after washing the membranes for 40 min.

its cause, PEG600 has an affinity to water, so it is easy to flow out into the coagulation bath, leading to no effect on hydrophilicity of neat CPVC membrane. However, contact angles of CPVC/Al_2O_3 membrane, CPVC/TiO_2 membrane, CPVC/ZnO membrane, and CPVC/SiO_2 membrane decreased after adding PEG. As for its cause, as the amount of the nanoparticle reaches 3 wt.%, nanoparticles agglomerate on the membrane surface, reducing the contact area of the hydroxyl carried by nanoparticles [37,40,41], but the contact area of hydroxyl increased after adding PEG, resulting from PEG weakening the surface tension of the casting solution and thus facilitating the uniform dispersion of nanoparticles, leading to the increased hydrophilicity and the decreased contact angle.

3.5. Antifouling properties

The membrane antifouling performance was evaluated with deionized water and BSA aqueous solutions as model foulants. The antifouling data are shown in Figs. (8)–(10), which contained the variation of different additives. After the filtration of BSA solution, the R_{ir} could not be recovered by simple hydraulic cleaning, indicating the irreversible adsorption and adhesion of foulants on membrane surface. Moreover, the R_r could be recovered by hydraulic cleaning, indicating the reversible foulant deposition and weak interaction between foulants and membrane surface. The FRR was the characteristic index, the higher the FRR means the better antifouling performance of the membranes.

For investigating this antifouling performance, PWF of the membranes should be calculated after they have been in contact with foulant agents. Therefore, PWF before and after being in contact with BSA has been measured and compared, and the results are shown in Fig. 8. Permeation results indicate that in all the steps, they follow a similar trend. They usually start with higher flux, and after a while, they become steady. PWF is much more than flux of feed containing 1.0 g mL^{-1} BSA, thereby membranes are more permeable for water than BSA. However, as BSA passes through the membranes, it can interact with internal surface and form a layer on them. This will result in lower flux due to increased resistance.

The FRR data and filtration resistances are shown in Figs. 9 and 10. FRR of neat CPVC membrane increased after adding nanoparticles. Simultaneously, R_t and R_{ir} of neat CPVC membrane decreased and R_r increased after adding nanoparticles. Due to the addition of nanoparticles, the hydrophilicity of CPVC membrane was improved and the rejection between membrane surface and BSA molecules was enhanced. However, FRR of neat CPVC membrane did not change after adding PEG. Meantime, R_t and R_r of neat CPVC membrane hardly changed, and R_{ir} did not change after adding PEG. As discussed in contact angle, PEG600 has an affinity to water, so it is easy to flow out into the coagulation bath, leading to no effect on hydrophilicity of neat CPVC membrane. Subsequently, we can see that FRR of CPVC/Al_2O_3 membrane, CPVC/TiO_2 membrane, CPVC/ZnO membrane, and CPVC/SiO_2 membrane increased after adding PEG. Simultaneously, R_{ir} of CPVC/Al_2O_3 membrane, CPVC/TiO_2 membrane, CPVC/ZnO membrane, and CPVC/SiO_2 membrane decreased and R_r increased after adding PEG. As for its causes, due to nanoparticle aggregation, as the amount of the nanoparticle reaches 3 wt.% on the membrane surface, reducing the contact area of hydroxyl carried by nanoparticles, the rejection between membrane surface and BSA molecules is weakened. However, PEG weakens the surface tension of the casting solution, facilitating the uniform dispersion of nanoparticles, which leads to the increased contact area of hydroxyl, leading to increment in hydrophilicity and the increased antifouling properties.

3.6. Mechanical properties

The mechanical properties of neat CPVC membrane and all the modified membranes with different additives are shown in Fig. 11. As shown in Fig. 11, tensile strength of neat CPVC membrane increased after adding nano-Al_2O_3,

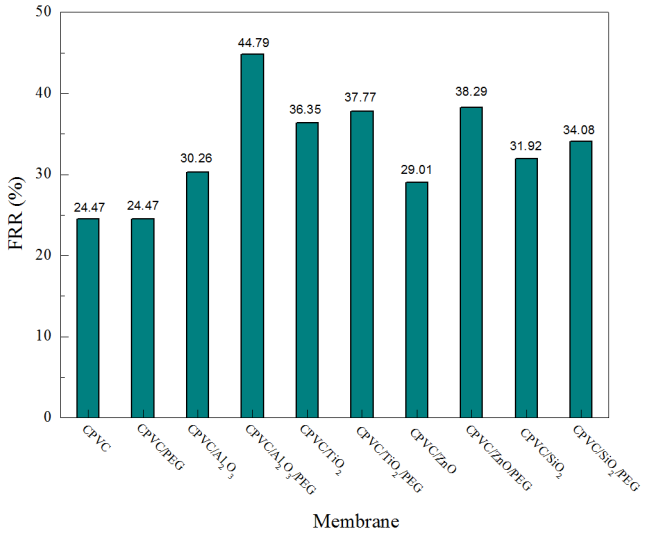

Fig. 9. Flux recovery ratio of neat CPVC membrane and all the modified membranes with different additives.

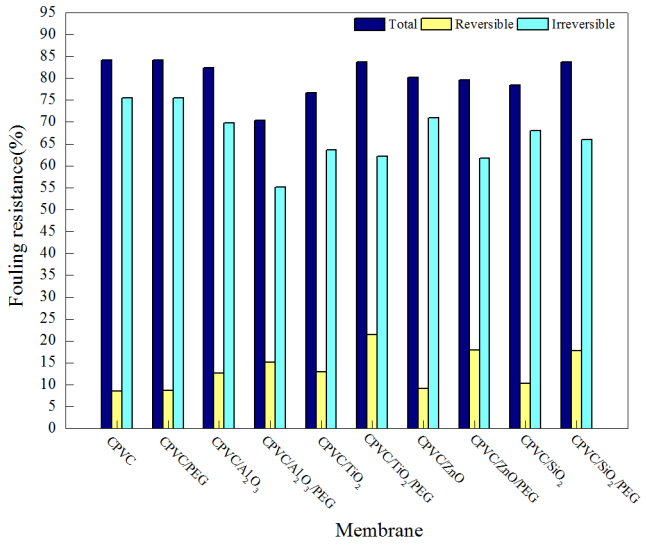

Fig. 10. Filtration resistances of neat CPVC membrane and all the modified membranes with different additives.

nano-TiO_2, and nano-ZnO and decreased after adding nano-SiO_2. Elongation of neat CPVC membrane decreased after adding nano-Al_2O_3, nano-TiO_2, and nano-SiO_2 and increased after adding nano-ZnO. As for its causes, on one hand, this is mainly due to the reinforcement effect of the nanoparticles and dispersion of the nanoparticles in membranes acts as physical cross-links to bear the stress of the load and, therefore, improve the membrane mechanical properties [42]. On the other hand, more nanoparticle dosage made membranes more rigid and weakened the mechanical properties of membranes because there was no strong affinity between CPVC and untreated nanoparticles [43]. Then, it can be seen that mechanical properties of neat CPVC membrane increased after adding PEG which may be related to the disappearance

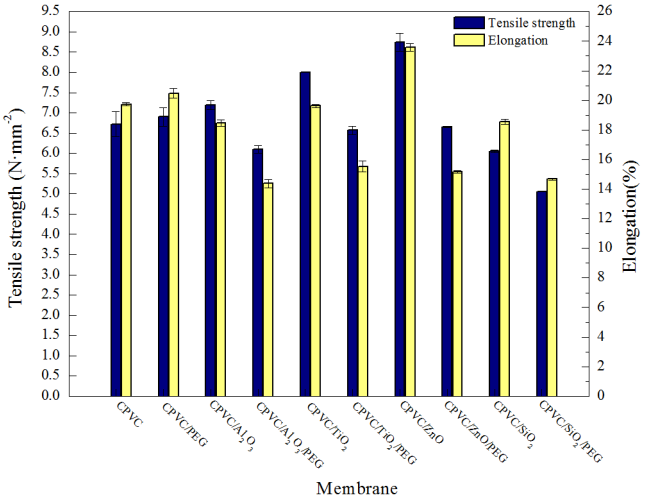

Fig. 11. Mechanical properties of neat CPVC membrane and all the modified membranes with different additives.

of cone hole. However, it can be seen that mechanical properties of CPVC/Al_2O_3 membrane, CPVC/TiO_2 membrane, CPVC/ZnO membrane, and CPVC/SiO_2 membrane decreased dramatically after adding PEG which may be related to a lot of micropores formed by the efflux of PEG.

4. Conclusions

In this paper, the effects of additives of nanoparticles (nano-Al_2O_3, nano-TiO_2, nano-ZnO, and nano-SiO_2), PEG, and nanoparticles/PEG on casting solution shear viscosity, morphology, and membrane performances of CPVC UF membrane were studied in detail. With the addition of PEG, the water flux increased dramatically, but the flux recovery rate did not change. With the addition of nanoparticles, the flux recovery rate increased, but the water flux and the rejection both declined. However, with the addition of PEG in CPVC/nanoparticle membranes, the water flux and the rejection were restored and the flux recovery rate further increased, among which flux recovery rate of CPVC/Al_2O_3 membrane increased to 44.79%. The flux recovery rate of CPVC/Al_2O_3/PEG membrane is much higher than other membranes. And the mechanical properties of CPVC/Al_2O_3/PEG are similar to those of other CPVC/nanoparticle/PEG membranes. Therefore, this paper considers that Al_2O_3/PEG composite additive is the best for CPVC membrane modification.

Acknowledgment

The authors thank the Donghua University (DHU, China) for all of the supports provided.

References

[1] H.C. Song, J.H. Shao, Y.L. He, B. Liu, X.Q. Zhong, Natural organic matter removal and flux decline with PEG-TiO_2-doped PVDF membranes by integration of ultrafiltration with photocatalysis, J. Membr. Sci., 405 (2012) 48–56.

[2] Y. Lu, S.L. Yu, B.X. Chai, X.D. Shun, Effect of nano-sized Al_2O_3-particle addition on PVDF ultrafiltration membrane performance, J. Membr. Sci., 276 (2006) 162–167.
[3] Y.N. Yang, J. Wu, Q.Z. Zhang, X.S. Chen, H.X. Zhang, The research of rheology and thermodynamics of organic-inorganic hybrid membrane during the membrane formation, J. Membr. Sci., 311 (2008) 200–207.
[4] R. Abedini, S.M. Mousavi, R. Aminzadeh, A novel cellulose acetate (CA) membrane using TiO_2 nanoparticles: preparation, characterization and permeation study, Desalination, 277 (2011) 40–45.
[5] N. Maximous, G. Nakhla, K. Wong, W. Wan, Optimization of Al_2O_3/PES membranes for wastewater filtration, Sep. Purif. Technol., 73 (2010) 294–301.
[6] A.M. Bazargan, Z. Gholamvand, M. Naghavi, M.R. Shayegh, S.K. Sadrnezhaad, Phase inversion preparation and morphological study of polyvinylidene fluoride ultrafiltration membrane modified by nano-sized alumina, World Scientific Publ. Co., Funct. Mater. Lett., 2 (2009) 113–119.
[7] Y. Lu, H. Sun, L.L. Meng, S.L. Yu, Application of the Al_2O_3-PVDF nanocomposite tubular ultrafiltration (UF) membrane for oily wastewater treatment and its antifouling research, Sep. Purif. Technol., 66 (2009) 347–352.
[8] J. Garcia-Ivars, M.I. Iborra-Clar, M.I. Alcaina-Miranda, J.A. Mendoza-Roca, L. Pastor-Alcaniz, Treatment of table olive processing wastewaters using novel photomodified ultrafiltration membranes as first step for recovering phenolic compounds, J. Hazard Mater., 290 (2015) 51–59.
[9] M.R. Mehrnia, Y.M. Mojtahedi, M. Homayoonfal, What is the concentration threshold of nanoparticles within the membrane structure? A case study of Al_2O_3/PSf nanocomposite membrane, Desalination, 372 (2015) 75–88.
[10] R.A. Damodar, S.J. You, H.H. Chou, Study the self cleaning, antibacterial and photocatalytic properties of TiO_2 entrapped PVDF membranes, J. Hazard. Mater., 172 (2009) 1321–1328.
[11] Q.Y. Wang, Z.W. Wang, J. Zhang, J. Wang, Z.C. Wu, Antifouling behaviours of PVDF/nano-TiO_2 composite membranes revealed by surface energetics and quartz crystal microbalance monitoring, RSC Adv., 4 (2014) 43590–43598.
[12] A. Sotto, A. Boromand, S. Balta, J. Kim, B. Van der Bruggen, Doping of polyethersulfone nanofiltration membranes: antifouling effect observed at ultralow concentrations of TiO_2 nanoparticles, J. Mater. Chem., 21 (2011) 10311–10320.
[13] A.W. Qin, X. Li, X.Z. Zhao, D. Liu, C. He, Engineering a highly hydrophilic PVDF membrane via binding TiO_2 nanoparticles and a PVA layer onto a membrane surface, ACS Appl. Mater. Interfaces, 7 (2015) 8427–8436.
[14] S.B. Mishra, S. Sachan, P.K. Mishra, M.R. Ramesh, Preparation and characterization of PPEES-TiO_2 composite microporous UF membrane for oily water treatment, Procedia Mater. Sci., 5 (2014) 123–129.
[15] J.M. Hong, Y. He, Polyvinylidene fluoride ultrafiltration membrane blended with nano-ZnO particle for photo-catalysis self-cleaning, Desalination, 332 (2014) 67–75.
[16] S. Balta, A. Sotto, P. Luis, L. Beneab, B. Van der Bruggena, J. Kimd, A new outlook on membrane enhancement with nanoparticles: the alternative of ZnO, J. Membr. Sci., 389 (2012) 155–161.
[17] L.G. Shen, X.K. Bian, X.F. Lu, L.Q. Shi, Z.Y. Liu, L.F. Chen, Z.C. Hou, K. Fan, Preparation and characterization of ZnO/polyethersulfone (PES) hybrid membranes, Desalination, 293 (2012) 21–29.
[18] Y. Jafarzadeh, R. Yegani, M. Sedaghat, Preparation, characterization and fouling analysis of ZnO/polyethylene hybrid membranes forcollagen separation, Chem. Eng. Res. Des., 94 (2015) 417–427.
[19] S. Zhao, W.T. Yan, M.Q. Shi, Z. Wang, J.X. Wang, S.C. Wang, Improving permeability and antifouling performance of polyethersulfone ultrafiltration membrane by incorporation of ZnO-DMF dispersion containing nano-ZnO and polyvinylpyrrolidone, J. Membr. Sci., 478 (2015) 105–116.
[20] Z.J. Yu, X.Y. Liu, F.B. Zhao, X.Y. Liang, Y. Tian, Fabrication of a low-cost nano-SiO_2/PVC composite ultrafiltration membrane and its antifouling performance, J. Appl. Polym. Sci., 132 (2015) 1–11.
[21] S. Habibi, A. Nematollahzadeh, Enhanced water flux through ultrafiltration polysulfone membrane via addition-removal of silica nano-particles: synthesis and characterization, J. Appl. Polym. Sci., 133 (2016) 1–9.
[22] J.N. Shen, H.M. Ruan, L.G. Wu, C.J. Gaoc, Preparation and characterization of PES-SiO_2 organic-inorganic composite ultrafiltration membrane for raw water pretreatment, Chem. Eng. J., 168 (2011) 1272–1278.
[23] X. Huang, J. Zhang, W.P. Wang, Y.D. Liu, Z.B. Zhang, L. Li, W.L. Fan, Effects of PVDF/SiO_2 hybrid ultrafiltration membranes by sol–gel method for the concentration of fennel oil in herbal water extract, RSC Adv., 5 (2015) 18258–18266.
[24] J. Zhu, X.Z. Zhao, C.J. He, Zwitterionic SiO_2 nanoparticles as novel additives to improve the antifouling properties of PVDF membranes, RSC Adv., 5 (2015) 53653–53659.
[25] Q. Li, S.L. Pan, X. Li, C. Liu, J.S. Li, X.Y. Sun, J.Y. Shen, W.Q. Han, L.J. Wang, Hollow mesoporous silica spheres/polyethersulfone composite ultrafiltration membrane with enhanced antifouling property, Colloids Surf. A, 487 (2015) 180–189.
[26] Y. Lu, S.L. Yu, B.X. Chai, Preparation of poly (vinylidene fluoride) (PVDF) ultrafiltration membrane modified by nano-sized alumina (Al_2O_3) and its antifouling research, Polymer, 46 (2005) 7701–7706.
[27] F. Liu, M.R.M. Abed, K. Li, Preparation and characterization of poly (vinylidene fluoride) (PVDF) based ultrafiltration membranes using nano γ-Al_2O_3, J. Membr. Sci., 366 (2011) 97–103.
[28] H. Rabiee, V. Vatanpour, M.H.D.A. Farahani, H. Zarrabi, Improvement in flux and antifouling properties of PVC ultrafiltration membranes by incorporation of zinc oxide (ZnO) nanoparticles, Sep. Purif. Technol., 156 (2015) 299–310.
[29] J. Zhang, Z.W. Wang, X.R. Zhang, X. Zheng, Z.C. Wu, Enhanced antifouling behaviours of polyvinylidene fluoridemembrane modified through blending with nano-TiO_2/polyethyleneglycol mixture, Appl. Surf. Sci., 345 (2015) 418–427.
[30] J. Garcia-Ivars, M.I. Alcaina-Miranda, M.I. Iborra-Clar, J.A. Mendoza-Roca, L. Pastor-Alcaniz, Enhancement in hydrophilicity of different polymer phase-inversion ultrafiltration membranes by introducing PEG/Al_2O_3 nanoparticles, Sep. Purif. Technol., 128 (2014) 45–57.
[31] M. Ali, M. Zafar, T. Jamil, M.T.Z. Buff, Influence of glycol additives on the structure and performance of cellulose acetate/zinc oxide blend membranes, Desalination, 270 (2011) 98–104.
[32] G. Arthanareeswaran, T.K. Sriyamuna Devi, D. Mohan, Development, characterization and separation performance of organic-inorganic membranes: Part II. Effect of additives, Sep. Purif. Technol., 67 (2009) 271–281.
[33] M. Higashi, J. Morita, N. Shimada, T. Kitagawa, Long-term-hydrophilic flat-sheet microfiltration membrane made from chlorinated poly (vinyl chloride), J. Membr. Sci., 500 (2016) 180–189.
[34] M.S. Muhamad, M.R. Salim, W.J. Lau, Surface modification of SiO_2 nanoparticles and its impact on the properties of PES-based hollow fiber membrane, RSC Adv., 5 (2015) 58644–58654.
[35] I.C. Kim, K.H. Lee, Effect of poly (ethylene glycol) 200 on the formation of a polyetherimide asymmetric membrane and its performance in aqueous solvent mixture permeation, J. Membr. Sci., 230 (2004) 183–188.
[36] P. van de Witte, P.J. Dijkstra, J.W.A. van den Berg, J. Feijen, Phase separation processes in polymer solutions in relation to membrane formation, J. Membr. Sci., 117 (1996) 1–31.
[37] H. Rabiee, M.H.D.A. Farahani, V. Vatanpour, Preparation and characterization of emulsion poly(vinyl chloride) (EPVC)/TiO_2 nanocomposite ultrafiltration membrane, J. Membr. Sci., 472 (2014) 185–193.
[38] V. Vatanpour, S.S. Madaeni, A.R. Khataee, E. Salehi, S. Zinadini, H.A. Monfared, TiO_2 embedded mixed matrix PES nanocomposite membranes: influence of different sizes and types of nanoparticles on antifouling and performance, Desalination, 292 (2012) 19–29.

[39] N.A.A. Hamid, A.F. Ismail, T. Matsuura, A.W. Zularisam, W.J. Lau, E. Yuliwati, M.S. Abdullah, Morphological and separation performance study of polysulfone/titanium dioxide (PSF/TiO_2) ultrafiltration membranes for humic acid removal, Desalination, 273 (2011) 85–92.
[40] M.R. Esfahani, J.L. Tyler, H.A. Stretz, M.J.M. Wells, Effects of a dual nanofiller, nano-TiO_2 and MWCNT, for polysulfone-based nanocomposite membranes for water purification, Desalination, 372 (2015) 47–56.
[41] Y. Wei, H.Q. Chu, B.Z. Dong, X. Li, S.J. Xia, Z.M. Qiang, Effect of TiO_2 nanowire addition on PVDF ultrafiltration membrane performance, Desalination, 272 (2011) 90–97.
[42] Y. Jafarzadeh, R. Yegani, S.B. Tantekin-Ersolmaz, Effect of TiO_2 nanoparticles on structure and properties of high density polyethylene membranes prepared by thermally induced phase separation method, Polym. Adv. Technol., 26 (2015) 392–398.
[43] F.M. Shi, Y.X. Ma, J. Ma, P.P. Wanga, W.X. Suna, Preparation and characterization of PVDF/TiO_2 hybrid membranes with different dosage of nano-TiO_2, J. Membr. Sci., 389 (2012) 522–531.